Effects of single particle on shape phase transitions and phase coexistence in odd-even nuclei *

Xiang-Ru Yu(于向茹) Jing Hu(胡静) Xiao-Xue Li(李晓雪) Si-Yu An(安思雨) Yu Zhang(张宇)[1)]
Department of Physics, Liaoning Normal University, Dalian 116029, China

Abstract: A classical analysis of shape phase transitions and phase coexistence in odd-even nuclei has been performed in the framework of the interacting boson-fermion model. The results indicate that the effects of a single particle may influence different types of transitions in different ways. Especially, it is revealed that phase coexistence can clearly emerge in the critical region and thus be taken as a indicator of the shape phase transitions in odd-even nuclei.

Keywords: shape phase transition, phase coexistence, the interacting boson-fermion model

PACS: 21.60.Fw, 21.60.Ev, 21.10.Gv **DOI:** 10.1088/1674-1137/42/3/034103

1 Introduction

Quantum phase transitions in nuclei have attracted a lot of attention in the past two decades [1–9]. Quantum phase transitions in nuclei are not of the usual thermodynamic type, but are related to changes in the ground state shapes of nuclei at zero temperature, hence the name "shape phase transitions" (SPTs) given to them. Most of the work related to SPTs has been carried out for even-even nuclei, using either the Bohr-Mottelson model [10] or the interacting boson model (IBM) [11]. Based on these two models, some important concepts related to quantum phase transitions, such as the triple point [12] and shape/phase coexistence [13], have been tested. In recent years, studies of SPTs have been extended to odd-even nuclei [14–30], and signals of phase transitions and phase coexistence have been clearly revealed [25]. A theoretical tool suitable for studying odd-even nuclei is the interacting boson-fermion model (IBFM) [31]. In this model, an odd-even nucleus is approximately considered as an odd-even system with an even-even core (boson) coupled to a single particle (fermion). Previous studies of SPTs in the IBFM focused on either the spherical to prolate transitions [20, 22] or the spherical to the γ-unstable transitions [16, 17, 21].

In this work, we will present a systematic analysis of the effects of a single particle on spherical to deformed SPTs in the IBFM, with the deformed shapes including the prolate, oblate and the deformed γ-unstable. Particularly, we will investigate how the presence of an odd particle can influence phase coexistence and triple point in odd-even systems.

2 Model Hamiltonian and shape phase diagram

2.1 Hamiltonian

The IBFM Hamiltonian can be generally written as

$$\hat{H}=\hat{H}_{\rm B}+\hat{H}_{\rm F}+\hat{V}_{\rm BF}, \tag{1}$$

where $\hat{H}_{\rm B}$ represents the boson core part, $\hat{H}_{\rm F}$ is the single particle part, and $\hat{V}_{\rm BF}$ represents the interactions between core and particle. Specifically, we consider the IBFM consistent-Q form [21]

$$\hat{H}=\varepsilon\left[(1-\eta)\hat{n}_d-\frac{\eta}{4N}\hat{Q}_{\rm BF}\cdot\hat{Q}_{\rm BF}\right], \tag{2}$$

where $\hat{n}_d=\sum_u d_u^\dagger d_u$ is the d boson number and

$$\hat{Q}_{\rm BF}\equiv\hat{Q}_{\rm B}^{\chi}+\hat{q}_{\rm F}, \tag{3}$$

is the total quadrupole operator with

$$\hat{Q}_{\rm B}^{\chi}=(d^\dagger s+s^\dagger\tilde{d})^{(2)}+\chi(d^\dagger\tilde{d})^{(2)} \tag{4}$$

being the boson quadrupole operator and

$$\hat{q}_{\rm F}=(a_j^\dagger\tilde{a}_j)^{(2)} \tag{5}$$

being the fermion quadrupole operator. In addition, η and χ are the control parameters with $\eta\in[0,1]$ and $\chi\in[-\sqrt{7}/2,\sqrt{7}/2]$, and ε is a scale factor, which will be set as 1 for convenience. From Eq. (2), it is easy to get

$$\hat{H}_{\rm B}=\left[(1-\eta)\hat{n}_d-\frac{\eta}{4N}\hat{Q}_{\rm B}^{\chi}\cdot\hat{Q}_{\rm B}^{\chi}\right], \tag{6}$$

Received 28 November 2017, Published online 29 January 2018
∗ Supported by National Natural Science Foundation of China (11375005)
1) E-mail: dlzhangyu_physics@163.com

which is actually the well-known consistent-Q Hamiltonian for the IBM [32]. One can also derive from Eq. (2)

$$\hat{V}_{\rm BF}=-\frac{\eta}{2N}Q_{\rm B}^{\chi}\cdot\hat{q}_{\rm F}, \tag{7}$$

which is quadrupole-quadrupole interaction between boson and fermion. As a result, the even-even core of the system in the present scheme is described by the IBM, while the effect of a single particle works through the quadrupole-quadrupole interaction between core and particle. It should be noted that the fermion part $H_{\rm F}$ contributes nothing but an additional constant to the ground state energy, since a fermion moving in a single-j shell case is supposed to be considered here. This term will thus be ignored in the following discussions for convenience.

2.2 Shape phase diagram for the boson system

In this section, we first give a brief discussion of the shape phase diagram described by Eq. (6). The Hamiltonian in Eq. (6) can be characterized by U(5) dynamical symmetry at the parameter point $(\eta,\chi)=(0,0)$, by O(6) dynamical symmetry at $(\eta,\chi)=(1,0)$, by SU(3) dynamical symmetry at $(\eta,\chi)=(1,-\frac{\sqrt{7}}{2})$, and by $\overline{\rm SU(3)}$ dynamical symmetry at $(\eta,\chi)=(1,\frac{\sqrt{7}}{2})$. To get the energy surfaces, one usually adopts the intrinsic state defined as [11]

$$|\beta,\gamma,N\rangle_{\rm B} = \frac{1}{\sqrt{N!(1+\beta^2)^N}}[s^\dagger+\beta\cos\gamma\ d_0^\dagger + \frac{1}{\sqrt{2}}\beta\sin\gamma(d_2^\dagger+d_{-2}^\dagger)]^N|0\rangle. \tag{8}$$

Then the energy surface corresponding to Eq. (6) is given by

$$V_{\rm B}(\beta,\gamma)\equiv\langle\beta,\gamma,N|\hat{H}_{\rm B}|\beta,\gamma,N\rangle_{\rm B}. \tag{9}$$

To determine the types and orders of the SPTs, one should minimize the energy surface $V_{\rm B}(\beta,\gamma)$ with respect to β and γ for given χ and η. Then one gets the ground state energy $E_{\rm g}\equiv V_{\rm B}(\eta,\chi,\beta_{\rm e},\gamma_{\rm e})$ with $\beta_{\rm e}$ and $\gamma_{\rm e}$ being the optimal values. For $\chi\neq 0$, one can prove that the γ-dependence in Eq. (9) gives either $\gamma_{\rm e}=0^\circ$ or $\gamma_{\rm e}=60^\circ$, but the results for $\gamma_{\rm e}=60^\circ$ can be equivalently obtained by taking $\gamma_{\rm e}=0^\circ$ and $\beta=-\beta_{\rm e}$ [11]. For $\chi=0$, one can prove that the energy surface in Eq. (9) is always γ-independent. Particularly, the deformed γ-unstable situation may correspond to the energy surface with a valley in γ ranging from 0° to 60°. In this case, one may get $V_{\rm B}(\eta,\chi=0,\beta_{\rm e})=V_{\rm B}(\eta,\chi=0,-\beta_{\rm e})$ and this feature can be taken to characterize the deformed γ-unstable shape. One should bear in mind that it does not mean that there are really two degenerate minima at $\pm\beta_{\rm e}$, but one can always use the energy curve obtained from Eq. (9) at $\gamma=0^\circ$ with two degenerate minima located symmetrically at $\pm\beta_{\rm e}$ to indicate the deformed γ-unstable shape, which is similar to the treatment in Ref. [21]. In short, by setting $\gamma=0^\circ$, it is shown that $\beta_{\rm e}=0$, $\beta_{\rm e}>0$, $\beta_{\rm e}<0$ and $\pm\beta_{\rm e}\neq 0$ represent the spherical, prolate, oblate and deformed γ-unstable case, respectively. Thus $\beta_{\rm e}$ is often considered as the classical order parameter for identification of different shapes as well as the SPTs among them [11].

For the 1st order SPT, $\beta_{\rm e}$ as a function of y is not continuous and jumps around the critical point $y_{\rm c}$ from one value to another, where y represents the control parameter η or χ. For the 2nd order SPT, $\beta_{\rm e}$ is continuous but $\frac{\partial\beta_{\rm e}}{\partial y}$ is not. According to these criteria, it can be found that the system described by Eq. (6) may experience 1st order SPTs at the critical points [33]

$$\eta_{\rm c}=\frac{28N}{56(N-1)+\chi^2(5+2N)} \tag{10}$$

with $\chi\in[-\sqrt{7}/2,\sqrt{7}/2]$, except for the U(5)-O(6) SPT occurring at the triple point $\eta_{\rm c}=N/2(N-1)$ [12], which is a 2nd order transition. In addition, the prolate to oblate transitions along the χ direction are also proven to be 1st order SPTs with $\chi_{\rm c}=0$ [12]. The two-dimensional parameter space of the IBM can be characterized by a symmetric triangle [12] as shown in Fig. 1, which covers all types of SPTs in the IBM up to two-body interactions. Here we focus on only the spherical to deformed SPTs with the deformed shape phases including the prolate, oblate and deformed γ-unstable. In the following sections, we will discuss the case with a single fermion moving in the $j=11/2$ shell coupled to the even-even core that undergoes the spherical to deformed SPTs mentioned above.

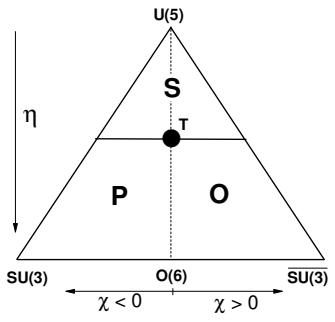

Fig. 1. Phase diagram in the IBM parameter space, where S represents the region with $\beta_{\rm e}=0$, corresponding to a spherical shape, P denotes the region with $\beta_{\rm e}>0$, corresponding to prolate deformation, and O represents the region with $\beta_{\rm e}<0$, corresponding to oblate deformation. In addition, the horizontal line represents the 1st-order transitional point, while the solid dot indicated by T denotes the triple point.

2.3 Energy surfaces for the boson-fermion system

To identify the SPTs in this boson-fermion system, one should adopt the intrinsic state for the coupled system [21, 22]

$$|\beta,\gamma,N;j,K\rangle_{\rm BF}=|\beta,\gamma,N\rangle_{\rm B}\otimes|j,K\rangle_{\rm F}. \tag{11}$$

We then diagonalize the total Hamiltonian (2) in this basis with $K=-j,\ -j+1,...,j$ to get the energy expectation values $E(\beta,\gamma)$. Here, we consider, for simplicity, the $\gamma=0^\circ$ case, which indicates that the quantum number K would be a good quantum number in this case. Due to the $K\leftrightarrow -K$ symmetry, the dimension of the basis space is $j+1/2$, which indicates that one only needs to consider positive values of K. If the single fermion effect is analogous to an external field to the boson core, $\gamma=0^\circ$ here means the field has an axial symmetry [22, 23]. Then the energy expectation values can be solved as

$$\begin{aligned} E(\beta)_K &= \frac{N\beta^2}{1+\beta^2}[(1-\eta)-(\chi^2+1)\frac{\eta}{4N}]-\frac{5N\eta}{4N(1+\beta^2)} \\ &- \frac{N\eta(N-1)}{4N(1+\beta^2)^2}[4\beta^2-4\sqrt{\frac{2}{7}}\chi\beta^3+\frac{2}{7}\chi^2\beta^4] \\ &+ \frac{\sqrt{5}\eta}{2}\frac{\beta}{1+\beta^2}(2-\beta\chi\sqrt{\frac{2}{7}})P_j[3K^2-j(j+1)] \end{aligned} \tag{12}$$

with $P_j=1/\sqrt{(2j-1)j(2j+1)(j+1)(2j+3)}$. Minimization of $E(\beta)_K$ with respect to β for given χ and η gives the optimal values $\beta_{\rm e}$, by which one can examine how the presence of a single fermion can influence different types of SPT. Notably, one should replace the dynamical symmetry G shown in Fig. 1 with G$\otimes$U($2j+1$) for the boson-fermion system, where G denotes U(5), O(6), SU(3) or $\overline{\rm SU(3)}$, because the fermion occupying a single j orbit may generate the dynamical symmetry U($2j+1$) [31].

3 SPTs in the boson-fermion system

Based on Eq. (12), the energy surfaces at typical parameter points and the evolutionary behaviors of the classical parameter have been extracted for different types of SPT, and the results are given in Figs. 2–6.

3.1 Spherical to prolate SPT

As seen in Fig. 2(a), the energy curves for different K have almost the same configurations as that for the even-even core, which indicates that the single fermion has little effect on the collective shape of the boson-fermion system in the spherical case. Similarly, the results in Fig. 2(c) indicate that the energy curves for different K are also similar to that for the even-even core with the

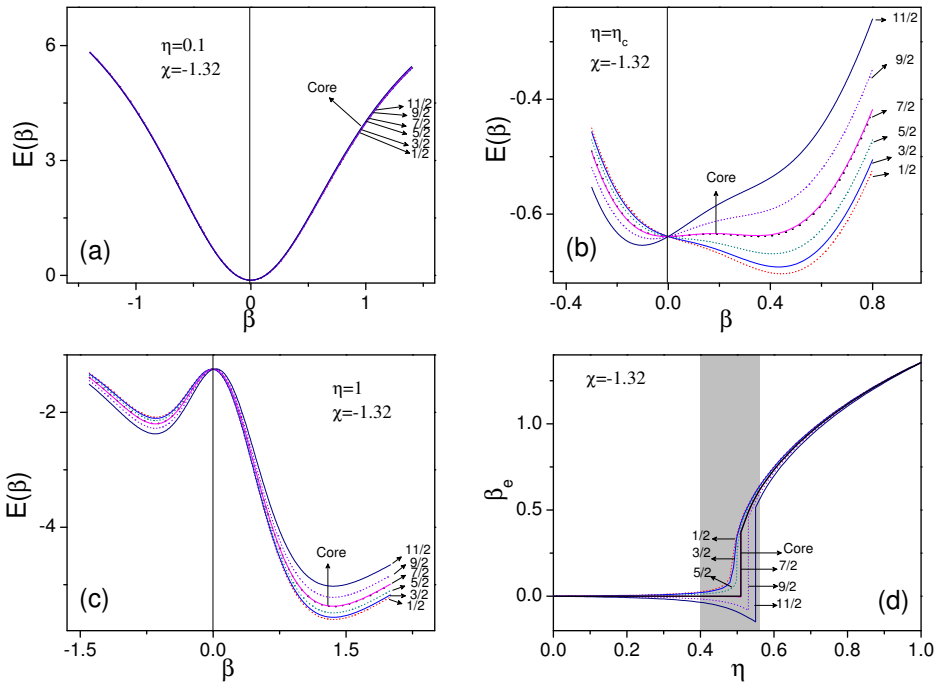

Fig. 2. (color online) Results related to the spherical to prolate SPT with $\chi=-1.32$. (a) Energy curves in the spherical case. (b) Energy curves at the critical point $\eta_{\rm c}$. (c) Energy curves in the prolate case. (d) Order parameter $\beta_{\rm e}$ as a function of η. In each panel, the curves denoted by 1/2, ..., 11/2 represent the cases with $K=1/2$, ..., 11/2, respectively, and "core" represents the results for the even-even core described by Eq. (9).

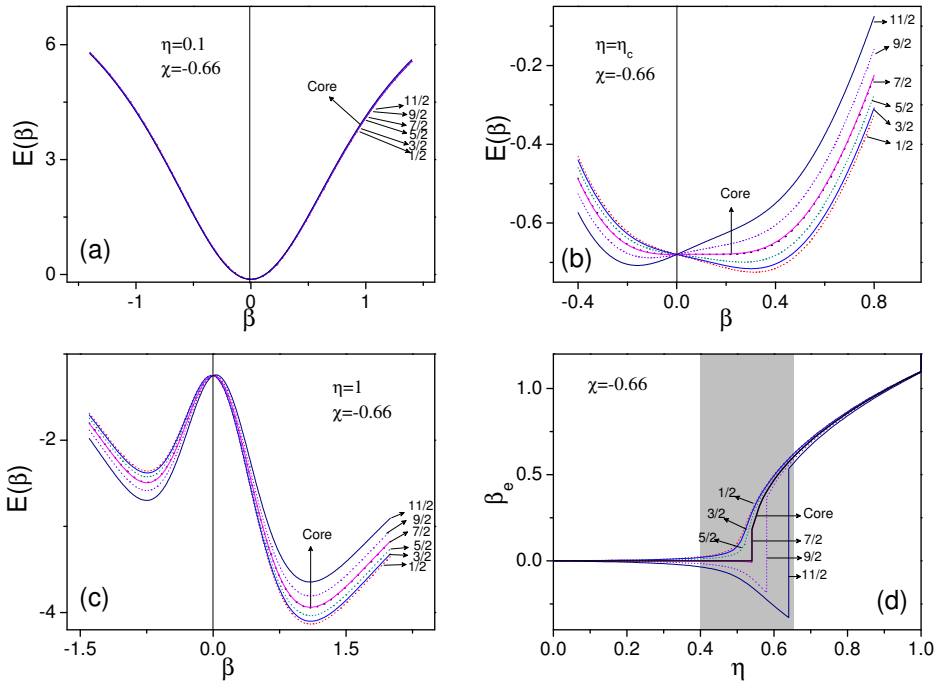

Fig. 3. (color online) Results related to the spherical to prolate SPT with $\chi=-0.66$. (a) Energy curves in the spherical case. (b) Energy curves at the critical point η_c. (c) Energy curves in the prolate case. (d) Order parameter β_e as a function of η. In each panel, the curves denoted by 1/2, ..., 11/2 represent the cases with $K=1/2$, ..., 11/2, respectively, and "core" represents the results for the even-even core described by Eq. (9).

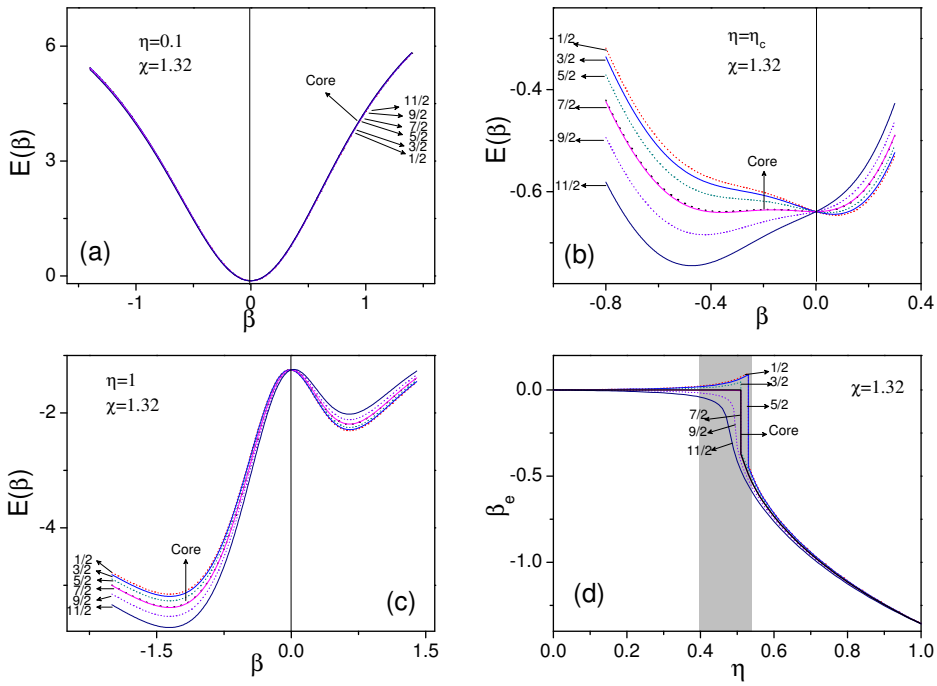

Fig. 4. (color online) Results related to the spherical to oblate SPT with $\chi=-1.32$. (a) Energy curves in the spherical case. (b) Energy curves at the critical point η_c. (c) Energy curves in the prolate case. (d) Order parameter β_e as a function of η. In each panel, the curves denoted by 1/2, ..., 11/2 represent the cases with $K=1/2$, ..., 11/2, respectively, and "core" represents the results for the even-even core described by Eq. (9).

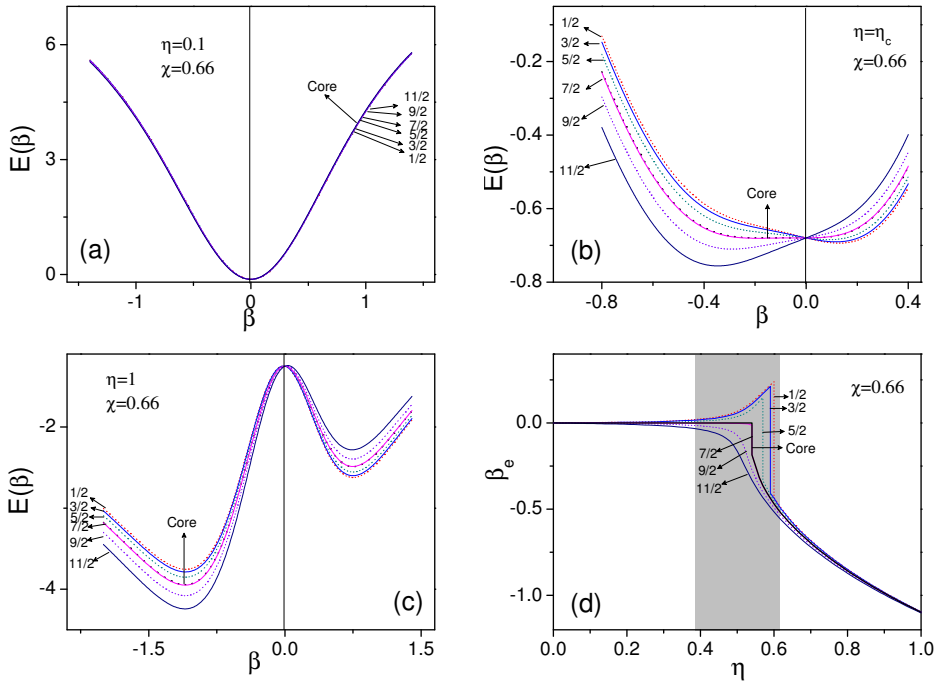

Fig. 5. (color online) Results related to the spherical to oblate SPT with $\chi=-0.66$. (a) Energy curves in the spherical case. (b) Energy curves at the critical point η_c. (c) Energy curves in the prolate case. (d) Order parameter β_e as a function of η. In each panel, the curves denoted by 1/2, ..., 11/2 represent the cases with $K=1/2$, ..., 11/2, respectively, and "core" represents the results for the even-even core described by Eq. (9).

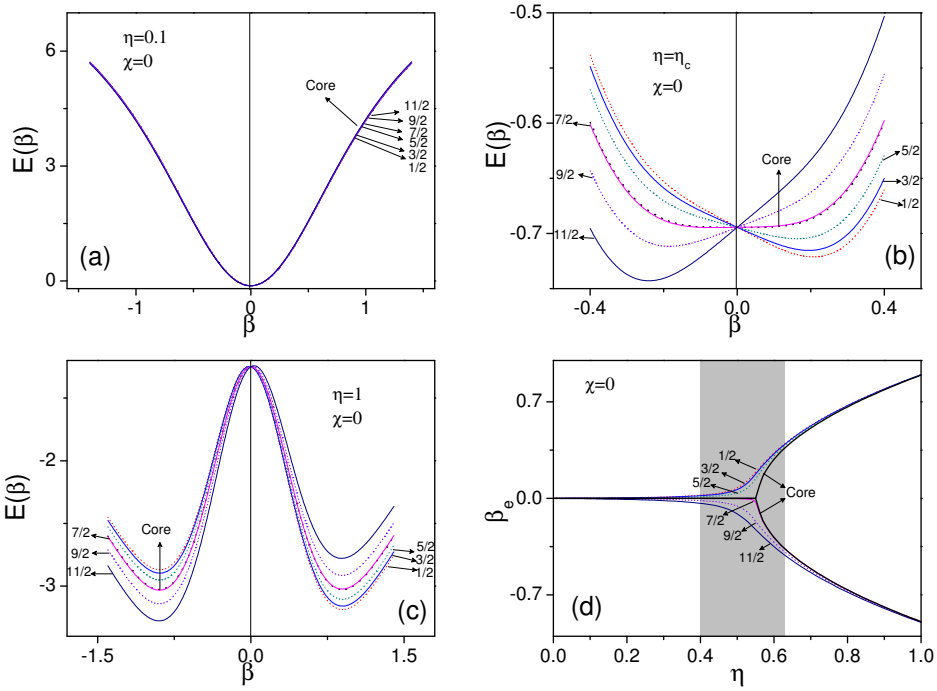

Fig. 6. (color online) Results related to the spherical to deformed γ-unstable SPT with $\chi=-0$. (a) Energy curves in the spherical case. (b) Energy curves at the critical point η_c. (c) Energy curves in the prolate case. (d) Order parameter β_e as a function of η. In each panel, the curves denoted by 1/2, ..., 11/2 represent the cases with $K=1/2$, ..., 11/2, respectively, and "core" represents the results for the even-even core described by Eq. (9).

corresponding minima all located at $\beta>0$. This means that the effect of the single fermion cannot change the shape of the system when the even-even core corresponds to a prolate deformation. For the situation at the critical point, one can derive from Fig. 2(b) that the energy curve for different K may have different configurations, thus indicating different types of deformation. Specifically, the cases for $K=1/2,\ 3/2,\ 5/2$ favor prolate deformation corresponding to $\beta_{\rm e}>0$, while the cases for $K=9/2,\ 11/2$ favor small oblate deformation with $\beta_{\rm e}<0$. In addition, the case for $K=7/2$ has almost the same energy curve configuration as the one for the even-even core, and both of them present two degenerate minima located at $\beta=0$ and $\beta>0$, respectively. Clearly, the results indicate that the boson-fermion system may allow multi-phase coexistence at the critical point. As further seen from Fig. 2(d), one can find that the effect of the single fermion is to weaken the transitional features for states with $K=1/2,\ 3/2,\ 5/2$ and to enhance them for states with $K=9/2,\ 11/2$. This feature was first revealed in Ref. [22]. In contrast, the state for $K=7/2$ may retain the same configuration as that for the even-even core. This point can be understood by seeing Eq. (12). The contribution of the last term in Eq. (12), which represents the effect of the single fermion, can be ignored in the case with $K=7/2$ and $j=11/2$, since $P_j[3K^2-j(j+1)]$ approaches zero in this case. In addition, the presence of the single fermion may induce a critical region (the grey color), in which $\beta_{\rm e}$ for different K rapidly changes with variation of η, in the coupled system, while the critical point $\eta_{\rm c}$ is just involved in the critical region, as seen in Fig. 2(d). All these features indicate that there should be more chances to identify shape/phase coexistence in odd-even nuclei near the critical point than in even-even nuclei. It should be noted that phase coexistence and shape coexistence are two different concepts in principle [13, 34]. Here we do not emphasize their differences but instead use the concept of phase coexistence to illustrate that different types of deformation induced by either single-particle excitation or collective excitation can coexist at the same parameter point ($\eta,\ \chi$).

To test the similar transitional situations in the inner area of the triangle phase diagram, we do the same calculations but for $\chi=-0.66$. The results are given in Fig. 3. As shown in Fig. 3, the energy surface configurations as well as the transitional features are very similar to those shown in Fig. 2, except that the effect of the single fermion may further enhance the transitional feature for large K values and meanwhile enlarge the range of the critical region (phase coexistence region). In short, phase coexistence in the boson-fermion system may become more pronounced when the parameter trajectories fall into the inner area of the triangle phase diagram shown in Fig. 1.

3.2 Spherical to oblate SPT

For the spherical to oblate SPTs, we will examine the results calculated for $\chi=1.32$, corresponding to the U(5)-$\overline{\rm SU(3)}$ leg, and those calculated for $\chi=0.66$, as an example for the inner area of the phase diagram. As shown in Fig. 4, the energy curves for different K in the spherical or oblate case may have configurations similar to that for the even-even core, which indicates that the presence of the single fermion cannot change the collective shape of the system in these two cases. In contrast, the energy curves at the critical point favor different types of deformation for different K values. This means that phase coexistence may also occur at the critical point for the spherical to oblate SPT. The evolutions of $\beta_{\rm e}$ shown in Fig. 4(d) further suggest that the effect of the single fermion in this case is to weaken the transitional features for states with large K ($K=11/2,\ 9/2$) but to enhance the features for states with small K ($K=1/2,\ 3/2,\ 5/2$), which is actually the inverse situation of those shown in Fig. 2 and Fig. 3. As expected, the state for $K=7/2$ shows the same transitional features as that for the even-even core. The results shown in Fig. 5 indicate that the transitional features and phase coexistence in this type of SPT will be further strengthened in the inner area of the triangle phase diagram.

3.3 Spherical to deformed γ-unstable SPT

As mentioned in Section 2, the γ-unstable deformation can be identified as the energy curve with two degenerate minima located symmetrically at $\pm\beta_{\rm e}$. For the spherical to deformed γ-unstable SPT, the related results corresponding to $\chi=0$ are given in Fig. 6. It should be noted that a classical analysis of the spherical to deformed γ-unstable SPT in the IBFM was previously given in Ref. [21] through the same Hamiltonian form with $j=9/2$, and the authors found that the transitional features could be smoothed out for all K values due to the effects of the odd fermion. Here we hope to revisit the this type of transition but with $j=11/2$, and to reveal the situations corresponding to more general j values. As shown in Fig. 6, the energy curves for all K values in the spherical case present the same features as that for the even-even core, while the results at $\eta_{\rm c}$ indicate clearly the coexistence of three shapes including spherical, prolate and oblate. It thus hints at a much clearer meaning of the triple point in odd-even systems than in even-even systems. In addition, the results in Fig. 6(c) indicate that the cases for large K favor oblate and those for small K favor prolate. In contrast, the energy curve for $K=7/2$ shows the same configuration as that for the even-even core with two degenerate minima located at $\pm\beta_{\rm e}$, thus indicating the deformed γ-unstable shape. One can further find from Fig. 6(d) that the effect of the single fermion in this case is to weaken the transi-

tional features for all K values relative to the even-even core, except for the case with $K=7/2$, for which the transitional features remain almost the same as for the even-even core.

It is not difficult to understand the above results, as well as those obtained in Ref. [21], by seeing Eq. (12), where one can find that $[3K^2-j(j+1)]$ will determine the sign of the last term of Eq. (12) and thus the intrinsic shape for a given K, since the first two terms in Eq. (12) with $\chi=0$ may generate either one minimum at $\beta_e=0$ or two degenerate minima at $\pm\beta_e\neq 0$. Specifically, one can derive that the cases with $K>\sqrt{j(j+1)/3}$ always favor oblate during the entire process of the spherical to γ-unstable SPT, while those with $K<\sqrt{j(j+1)/3}$ always favor prolate. In contrast, cases with $K\simeq\sqrt{j(j+1)/3}$ may maintain the same deformation as that for the even-even core. It thus explains why the spherical to γ-unstable SPT in the coupled system can be smoothed out for almost all the K values with given j. Accordingly, the $j=11/2$ case shown in Fig. 6 and the $j=9/2$ case considered in Ref. [21] provide two concrete examples for the above argument.

4 Summary

In summary, a classical analysis of SPTs and phase coexistence in odd-even nuclei has been given within the framework of the IBFM. The results indicate that the effects of the single particle may influence different types of SPT in different ways. Specifically, the transitional features in the spherical to prolate SPTs or the spherical to oblate SPTs may be enhanced for some states and weakened for others, except for the state with $K=7/2$, which has the same features the even-even core for all types of SPTs in the $j=11/2$ case. In contrast, the transitional features in the spherical to deformed γ-unstable SPT are smoothed out for almost all K values, which further confirms the analysis given in Ref. [21]. More importantly, it is revealed that more pronounced phase coexistence can emerge in the SPTs in odd-even systems near the critical point than in even-even systems, which suggests that phase coexistence can be taken as a robust signature of SPTs in odd-even nuclei. Although all the discussions in this work are based on the classical analysis of the IBFM, the related predictions can in principle be examined in experiments, as the IBFM has been proven to be a powerful theoretical tool to describe the spectroscopic properties of odd-A nuclei [27, 29–31]. For example, the effects of an odd particle on the STPs could be tested by checking the evolutionary features of some observables in odd-A nuclei relative to adjacent even-even nuclei, where the observables may include two-neutron separation energy [22, 23], odd-even mass difference [24], pairing excitation energy [26] or some specific E2 transitional rates [30].

It is worth mentioning that the present study is just a schematic illustration of the actual situation in odd-even nuclei, as we have confined our discussion to an odd-even system with the core coupled to a fermion within a single j shell via quadrupole-quadrupole interactions. A multi-j situation and more interaction terms such as exchange interaction and monopole interaction [31] may need to be taken into account to further prove or disprove the conclusions. Related work is in progress.

References

1 R. F. Casten and E. A. McCutchan, J. Phys. G, **34**: R285–R320 (2010)
2 P. Cejnar and J. Jolie, Prog. Part. Nucl. Phys., **62**: 210–256 (2009)
3 P. Cejnar, J. Jolie, and R. F. Casten, Rev. Mod. Phys., **82**: 2155–2212 (2010)
4 D. L. Zhang and Y. X. Liu, Chin. Phys. Lett., **20**: 1028–1030 (2003)
5 Y. X. Liu, L. Z. Mu, and H. Wei, Phys. Lett. B, **633**: 49–53 (2006)
6 Y. Sun, P. M. Walker, F. R. Xu et al, Phys. Lett. B, **659**: 165–169 (2008)
7 Y. A. Luo, Y. Zhang, X. Meng et al, Phys. Rev. C, **80**: 014311 (2009)
8 Z. P. Li, T. Nikšić, D. Vretenar et al, Phys. Rev. C, **81**: 034316 (2010)
9 Z. Zhang, Y. Zhang, Y. An et al, Chin. Phys. Lett., **30**: 102101 (2013)
10 A. Bohr and B. R. Mottelson, Nuclear Structure, Vol. 2 (Singapore: World Scientific, 1998)
11 F. Iachello and A. Arima, *The Interacting Boson Model* (England: Cambridge University, 1987)
12 J. Jolie, P. Cejnar, R. F. Casten et al, Phys. Rev. Lett., **89**: 182502 (2002)
13 F. Iachello, N. V. Zamfir, and R. F. Casten, Phys. Rev. Lett., **81**: 1191-1194 (1998)
14 J. Jolie, S. Heinze, P. Van Isacker et al, Phys. Rev. C, **70**: 011305(R) (2004)
15 F. Iachello, Phys. Rev. Lett., **95**: 052503 (2005)
16 C. E. Alonso, J. M. Arias, L. Fortunato et al, Phys. Rev. C, **72**: 061302(R) (2005)
17 C. E. Alonso, J. M. Arias, and A. Vitturi, Phys. Rev. C, **74**: 027301 (2006)
18 M. L. Liu, Phys. Rev. C, **76**: 054304 (2007)
19 C. E. Alonso, J. M. Arias, and A. Vitturi, Phys. Rev. Lett., **98**: 052501 (2007)
20 C. E. Alonso, J. M. Arias, L. Fortunato et al, Phys. Rev. C, **79**: 014306 (2009)
21 M. Böyükata, C. E. Alonso, J. M. Arias et al, Phys. Rev. C, **82**: 014317 (2010)
22 F. Iachello, A. Leviatan, and D. Petrellis, Phys. Lett. B, **705**: 379-382 (2011)
23 D. Petrellis, A. Leviatan, and F. Iachello, Ann. Phys., **326**: 926-957 (2011)
24 Y. Zhang, L. N. Bao, X. Guan et al, Phys. Rev. C, **88**: 064305 (2013)
25 Y. Zhang, F. Pan, Y. X. Liu et al, Phys. Rev. C, **88**: 014304 (2013)

26 Y. Zhang, X. Guan, Y. Wang et al, Chin. Phys. C, **39**: 104103 (2015)
27 K. Nomura, T. Nikšić, and D. Vretenar, Phys. Rev. C, **94**: 064310 (2016)
28 D. Bucurescu and N. V. Zamfir, Phys. Rev. C, **95**: 014329 (2017)
29 K. Nomura, T. Nikšić, and D. Vretenar, Phys. Rev. C, **96**: 014304 (2017)
30 K. Nomura, R. Rodríguez-Guzmán, and L. M. Robledo, Phys. Rev. C, **96**: 014314 (2017)
31 F. Iachello and P. Van Isacker, The Interacting Boson-Fermion Model (Cambridge: Cambridge University, 1991)
32 D. D. Warner and R. F. Casten, Phys. Rev. C, **28**: 1798–1805 (1983)
33 E. Williams, R. J. Casperson, and V. Werner, Phys. Rev. C, **81**: 054306 (2010)
34 K. Heyde, J. Jolie, R. Fossion et al, Phys. Rev. C, **69**: 054304 (2004)